J Mater Sci (2007) 42:1660–1672
DOI 10.1007/s10853-006-0907-9

Processing and behavior of nanostructured metallic alloys and composites by cryomilling

B. Q. Han · J. Ye · F. Tang · J. Schoenung · E. J. Lavernia

Received: 2 June 2006 / Accepted: 31 August 2006 / Published online: 9 January 2007

Abstract Recent interest in nanostructured materials stems, not only from their potential use in a variety of applications, but also from the reported discovery of novel fundamental phenomena. The consolidation of cryomilled powder provides a potential pathway towards large scale manufacturing of nanostructured metallic materials. This approach typically engenders the mechanical attrition of powders in liquid nitrogen, followed by consolidation, using established commercial techniques, such as isostatic pressing and extrusion. In this overview paper, published data are reviewed and discussed with particular emphasis on the following topics: nanostructure evolution mechanisms; primary consolidation and secondary processing methods; thermal stability of cryomilled materials; and mechanical behavior of consolidated materials. Recent mechanical behavior data and the associated mechanisms of cryomilled Al alloys are discussed in an effort to shed light into the fundamental behavior of ultrafine grained and nanostructured materials.

Introduction

The successful synthesis of large-scale bulk nanostructured materials with a grain size in the range of 10–200 nm represents a major achievement in the wide field of nanotechnology [1]. Large amounts of nanostructured metallic powders can be prepared by the approach of mechanical alloying [2], which involves the transformation of plasticity-induced dislocation structures into high angle grain boundaries. The end product of the milled powder is usually consolidated into fully dense nanocrystalline metallic compacts, which have unique physical and mechanical properties, as compared to those of their conventional counterparts.

Cryomilling is a variation of mechanical milling, in which metallic powders are milled in a cryogen (usually liquid nitrogen) slurry or at a cryogen temperature under processing parameters such that a nanostructured microstructure is attained [3–5]. Cryomilling takes advantage of both the extremely low cryogen temperature and the advantages that are provided with conventional mechanical milling. The extremely low milling temperature in cryomilling suppresses the recovery and recrystallization and leads to finer grain structures and more rapid grain refinement [2]. A number of recent studies report on the processing and behavior of nanostructured materials via cryomilling [6–10].

In this overview paper, the mechanisms that are responsible for the formation of a nanostructure during cryomilling are reviewed and subsequent consolidation techniques are discussed. More specifically, the present review addresses the following topics: cryomilling mechanisms; aluminum matrix composites processed by cryomilling; consolidation approaches; thermal stability of cryomilled materials; and mechanical behavior of consolidated materials. The mechanical behavior and the associated mechanisms of cryomilled Al alloys are discussed in an effort to shed light into the fundamental behavior of ultrafine grained and nanostructured materials.

B. Q. Han (✉) · J. Ye · F. Tang · J. Schoenung · E. J. Lavernia
Department of Chemical Engineering and Materials Science, University of California, Davis, CA 95616, USA
e-mail: bqhan@ucdavis.edu

Nanostructure powders via cryomilling

During mechanical alloying, the materials experience severe plastic deformation, resulting in grain refinement [11]. Powder evolution during the milling process involves five stages, i.e., particle flattening as a result of plastic deformation, welding dominance stage, equiaxed particle formation, random welding orientation of the powder particles and steady-state processing, during which a balance between fracturing and cold welding is established and microstructural refinement continues, as shown in Fig. 1 [12–14]. In view of the fact that severe plastic deformation during milling is a repeatable process, the milling time dominates the overall deformation strain. In order to obtain a microstructure with nanoscale grain sizes, adequate milling time is required.

Microscopically, the formation of nanocrystalline materials by mechanical alloying has been considered to evolve via three stages, as proposed by Fecht [11]. In the first stage, severe plastic deformation is applied to the powders during milling. This deformation is localized into shear bands containing a high density network of dislocations. The atomic level strain increases as a result of increasing dislocation density. In the second stage, due to the successive accumulation of dislocations in the microstructure, the large grains are disintegrated into subgrains that are separated by low-angle grain boundaries. The formation of these subgrains is attributed to the annihilation and recombination of dislocations, as well as the decrease of the atomic level strain. In the final stage, as milling time increases, further deformation leads to the formation of additional shear bands and an associated reduction of subgrain sizes, as well as the reorientation of final grains with high-angle misorientations.

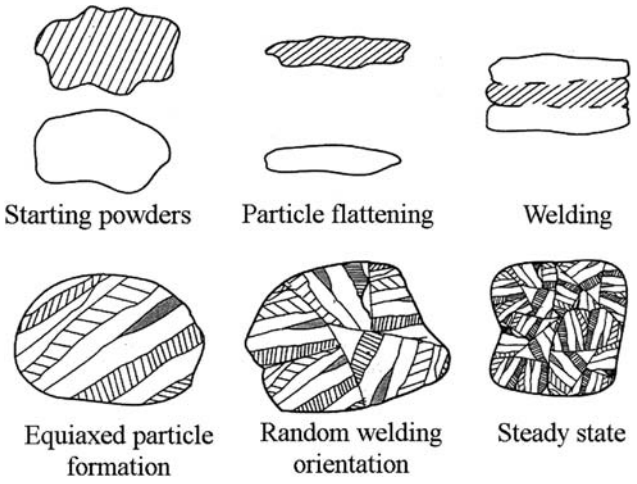

Fig. 1 The five stages of powder evolution during mechanical alloying [12–14]

Cooling of the milling media and powders is an effective approach to accelerating the fracture processes and quickly attaining steady-state conditions. There are several obvious advantages to cryomilling as compared to milling at room temperature. First, powder agglomeration and welding to the milling media are suppressed, resulting in a more efficient milling outcome (e.g., improved yield and microstructure refinement). Second, the oxidation during milling is significantly reduced under the protection of a nitrogen environment. Third, the milling time required to attain a nanostructure is significantly reduced, because the low temperature suppresses the annihilation of dislocations and the accumulation of a higher dislocation density is possible. As an example, a high density of dislocations of $1.7 \times 10^{17}/m^2$ was observed in a cryomilled Al–Mg alloy [5, 15], as shown in Fig. 2a. In addition, many dislocations appear as dipoles, which have been reported in many heavily deformed metals. The dipoles are in fact dislocation loops with elongation along one direction so that they look like a pair of single dislocations with opposite Burgers vectors. The density of dislocations in cryomilled Al–Mg alloys is much higher than that on cold-rolled Al–Mg alloys, which is usually in the range of $10^{15}/m^2$. In regions without dislocations, deformation twins, which are rarely observed in conventional aluminum alloys, have been frequently observed in cryomilled Al–Mg alloy, as shown in Fig. 2b. The existence of deformation twins are attributed to the severe plastic deformation introduced during milling, and not as a result of recrystallization [15].

The grain refinement process during milling is accomplished via the formation of shear bands under localized deformation and then the extension of shear bands to the entire sample [11]. The presence of elongated grains is often associated with insufficient milling time. Therefore, it would not be surprising to find microstructural features that manifest different relative degrees of deformation, and not simple lognormal distributions of randomly oriented equiaxed grains. In a cryomilled Al–7.5 wt.% Mg alloy after cryomilling for 8 h, two distinctive components of the microstructure, a random distribution of equiaxed grains between 10 and 30 nm diameter and elongated grains measuring 100–200 nm long by 30 nm wide, were revealed [5, 15], although the latter was less frequently observed, as shown in Fig. 3a, b. A similar microstructure with two distinctive components was also observed in several other cryomilled materials. It is interesting to note that the mean width of the

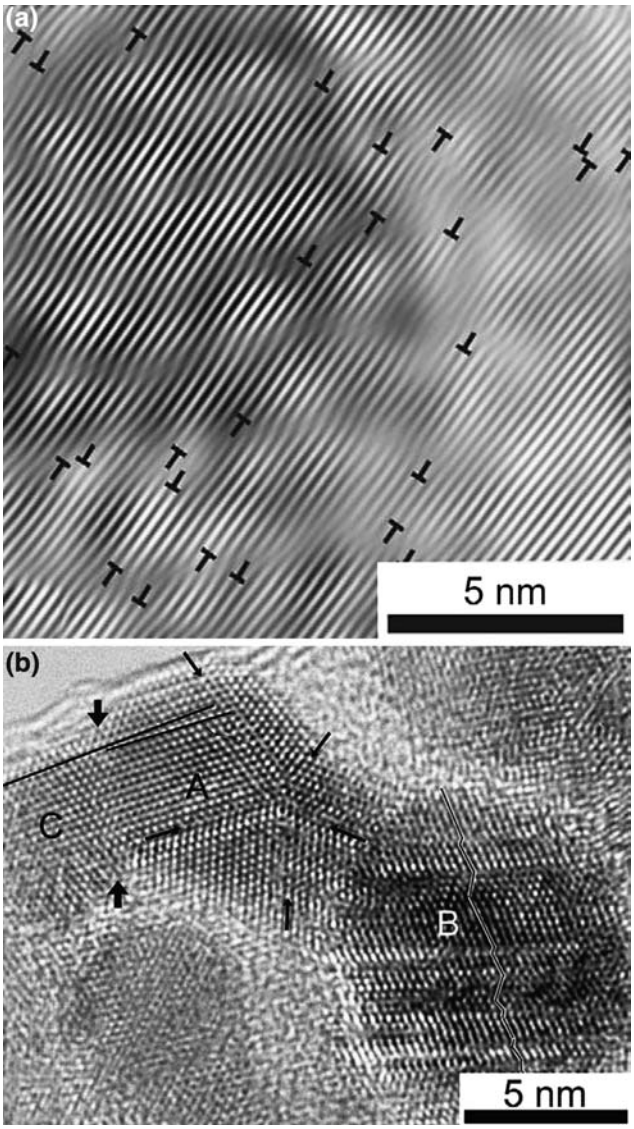

Fig. 2 Dislocations and deformation twins and stacking faults in a cryomilled Al–Mg alloy [5, 15]

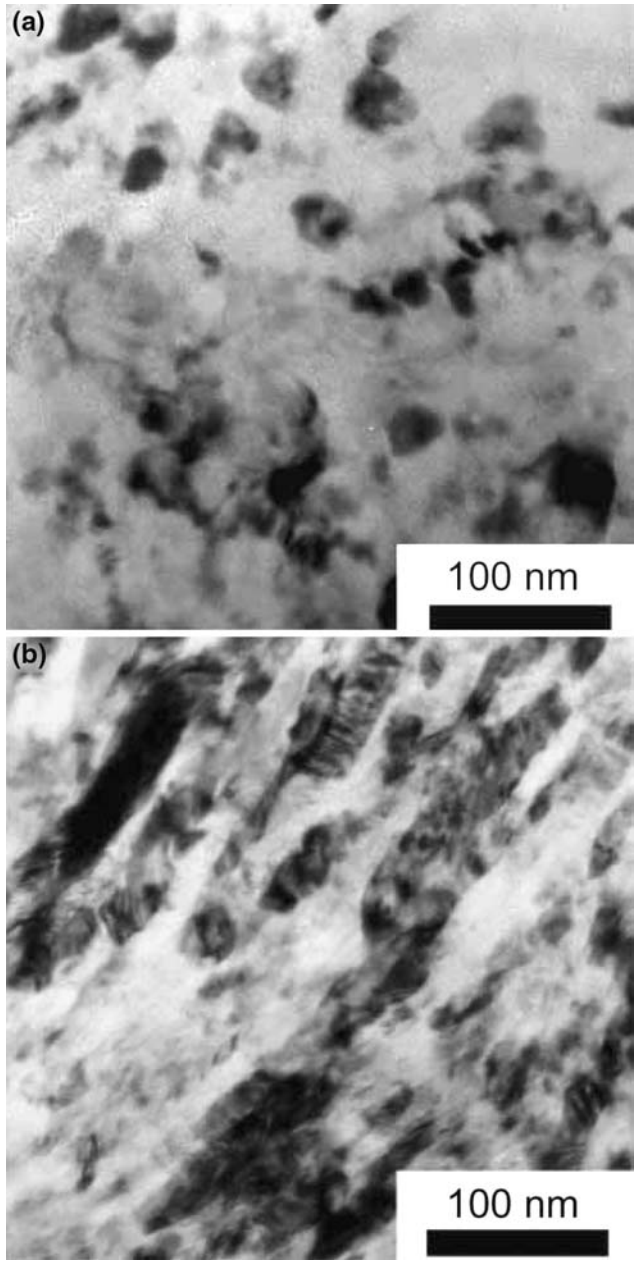

Fig. 3 (**a**) Frequently observed equiaxed grains and (**b**) less frequently observed elongated grains in a cryomilled Al–Mg alloy [5, 15]

elongated regions in cryomilled powder was essentially equal to the average grain size of equiaxed grains. With an increase of milling time, the grain size in a cryomilled Al–7.5%Mg alloy tends to decrease slowly to a saturated value, as shown in Fig. 4 [16].

Experimental and theoretical studies suggest that for each material, there is a minimum grain size that is obtainable by milling, and that its value is related to the intrinsic properties of the material [17]. Essentially, it has been proposed that the minimum grain size obtainable by milling scales inversely with the melting temperature or the bulk modulus. Mohamed recently developed a dislocation model to quantitatively describe the minimum grain size obtainable during milling [18]. According to this model, the minimum grain size is governed by a balance between the hardening rate introduced by dislocation generation and the recovery rate arising from dislocation annihilation and recombination. By balancing the rate of grain size decrease and the rate of grain size increase, the minimum grain size ($d_{\min}$) is given by [18]

$$d_{\min}/b = A_3 \exp(-\beta Q/4RT)(D_{\mathrm{PO}} G b^2/v_{\mathrm{o}} kT)^{0.25} (\gamma/Gb)^{0.5} (G/\sigma)^{1.25} \quad (1)$$

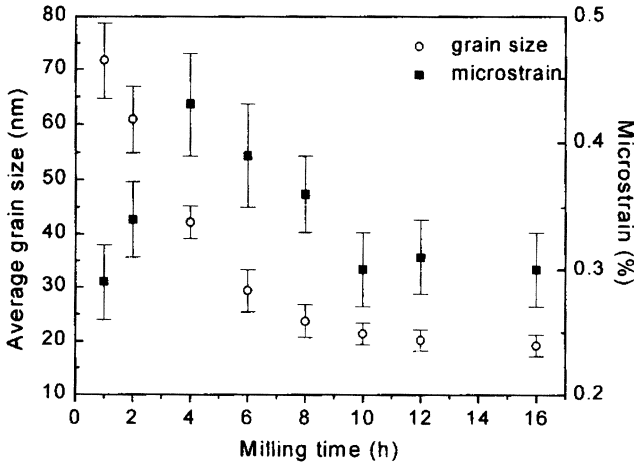

Fig. 4 The grain size and microstrain as a function of milling time in a cryomilled Al–7.5%Mg alloy [16]

where b is the value of Burgers vector, A_3 is a dimensionless constant, β is constant, Q is the self-diffusion activation energy, R is the gas constant, T is the absolute temperature, D_{PO} is the diffusion coefficient, G is the shear modulus, v_o is the initial dislocation velocity, k is Boltzmann's constant, γ is the stacking fault energy and σ is the applied stress. The model predicts that the minimum grain size scales inversely with hardness, proportionally with the stacking fault energy and exponentially with the activation energy for recovery. This model also predicts that the minimum grain size decreases with milling temperature.

During mechanical milling of a matrix/reinforcement mixture, the ductile matrix can still be deformed, flattened and cold welded in the same manner as in a monolithic metal; the presence of the hard reinforcement does not preclude grain refinement in the matrix, as discussed below [19]. Mechanical milling provides an advantage in that it eliminates the need for liquid or gaseous phases and high temperature processing, and therefore can prevent the formation of undesirable intermetallic phases that disrupt the interface and lead to poor mechanical properties. With mechanical milling the reinforcement particles are enfolded in the matrix material, which can eliminate the voids between the matrix and the ceramic reinforcement and potentially achieve solid state bonding between them. Ye et al. investigated the use of cryomilling to fabricate Al/B_4C composite powder [19] (and subsequent bulk samples [20]) as an alternative to conventional high-temperature infiltration methods. Interfacial phases normally observed were not seen in either the powder or the consolidated bulk material, as indicated by arrows in Fig. 5.

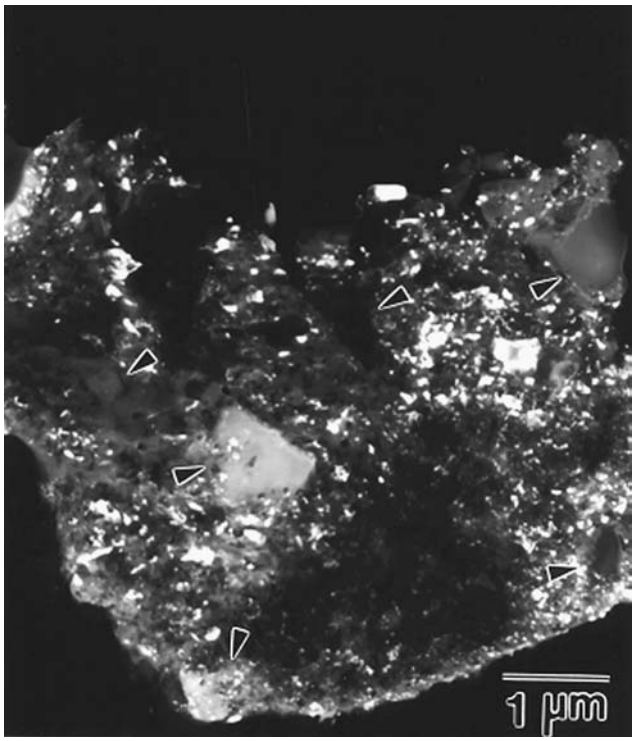

Fig. 5 Microstructure of cryomilled 5083 Al composite powders with 10% B_4C particles [19]

Another advantage of the mechanical milling technique as a method to synthesize metal matrix composite powders is the ability to provide a homogeneous distribution of the reinforcement in the matrix. Conventional blending methods often lead to clustering of the reinforcement, which can lead to poor mechanical behavior. Studies with both nanometric and micron-sized reinforcements indicate that homogeneous distributions of the reinforcement in the matrix can easily be achieved by using cryomilling [19, 21]. Figure 5 demonstrates that the reinforcement did not cluster in the Al/B_4C cryomilled powder; the nanostructured grains in the 5083 Al matrix can also be observed.

The presence of hard particles can affect the fracturing process (e.g., facilitate fracture) and thus the process of grain refinement in the metal matrix. As a consequence, a shorter milling time may be required to attain steady state conditions during milling. Chung et al. [22] reported that a small introduction of AlN particles with an initial size of 2 μm into Ni facilitated the grain refinement process for Ni during cryomilling, greatly reducing the Ni grain size from 132 nm for pure Ni down to 65 and 37 nm for Ni with 0.5 and 2.0 wt.% AlN, respectively, after milling for 8 h. During cryomilling, the AlN particles fractured into nanoscaled particles, from 2 μm down to 20–300 nm. This enhancement in the grain refinement process for the

Ni matrix was interpreted on the basis of a mechanism involving the interactions of dislocations with fractured small hard particles, and the thermally induced dislocation generation due to the difference in thermal expansion coefficient between matrix and reinforcement [22].

In a related study, however, Ye et al. [19] observed that the Al alloys with different contents of B_4C (0–25 wt.%) produced relatively invariable Al grain sizes (25 nm) after 8 h of cryomilling, which indicates that the existence of B_4C has an insignificant effect on the nanostructure formation of the Al matrix. In that study, the change in size of the B_4C particles was small, from 1–7 μm down to 0.2–2 μm. Similar reinforcement behavior has been observed for Si_3N_4, where the size of the Si_3N_4 changed from 8.6 to 1 μm after the mechanical milling of Al/Si_3N_4 [23]. In contrast, the size of AlN can decrease to 30 nm after the cryomilling of Ni/AlN and Al/AlN [23] and SiC particles were reduced to an average size of ~1 μm from an original size of 100 μm [23]. These studies indicate that the influence of reinforcements on the matrix grain refinement and of the cryomilling process itself on the reinforcement refinement is complex. The matrix grain refinement is also influenced by the intrinsic properties of the matrix, such as the minimum grain size obtainable during milling [18].

Consolidation of cryomilled powders

Widespread application of nanostructured metallic powders requires effective methods of consolidation to produce useful shapes, of sufficient size, with close to 100% theoretical density and maximum level of bonding between powder particles [24–26]. There are several approaches currently being employed to consolidate the nanostructured metallic and composite powders, such as hot isostatic pressing (HIP), cold isostatic pressing (CIP), Ceracon forging, spark plasma sintering (SPS), ultra high pressures (UHP) during pressing, and shock consolidation, as well as others. The final microstructure of the material in a form suitable for application depends not only on the milling parameters, but also on the method used to consolidate the powder. Several currently employed approaches for making large-scale cryomilled materials are discussed as follows.

Beginning with the earliest work [3], the most common primary consolidation route has been hot isostatic pressing (HIP). The densification of the HIP process has been described as a three-step process, beginning with loose packing of powder in the can, elimination of connected porosity due to the growth of necks at contact points between adjacent particles, and reduction of the size of individual pores [27, 28]. The growth of necks and filling in of pores at each stage is accomplished by a combination of plastic deformation of the powder particles, power-law creep, and mass diffusion to the remaining free surfaces. The driving force to achieve densification is associated with the reduction of surface area and, hence, surface energy of the pores. The pressure and temperature are two critical parameters for consolidation [26]. Since the consolidation of the milled powder usually requires high temperatures for long time, there is a challenge for retaining nanoscale grain size. In the case of HIP consolidation, diffusional processes can lead to micron-size grains forming in the triple-point areas between the nano-grained prior powder particles [21, 29]. Recently, cold isostatic pressing (CIP) has been employed to compact the cryomilled powders [9, 20, 30]. Although CIP is operated under a much higher isostatic pressure than that in HIP, the particle bonding due to diffusion in CIP is much weaker.

Ceracon forging [31–33], a quasi-isostatic forging with a relative high speed (lasting only several seconds), can enable both consolidation and impart shear stresses to improve ductility, removing the need for HIP, and thus is very attractive for larger scale consolidation. The process uses a heated granular pressure-transmitting medium to achieve full density in green compacts that are rapidly heated to the desired consolidation temperatures. As a cost competitive alternative to HIP, the Ceracon forging of canned powders can be used as an effective preparation step for secondary operations such as hot extrusion, rolling and superplastic forming. Ceracon forging can also be used to produce small near-net shape forms of rapidly solidified metal powders and metal/ceramic particulates using a conventional forging press [32].

Although nearly full density is attainable in the consolidated materials, the ductility of the materials processed via isostatic pressing is generally low [34]. This is due to the presence of prior particle boundaries, usually decorated with a surface oxide, that are not removed by isostatic deformation. In addition, small amounts of porosity usually exist after the primary consolidating step. To break up the prior particle boundaries, a shear stress needs to be applied to the material. Therefore, secondary processing, such as extrusion, rolling or forging is necessarily performed. Recent attempts involving the combination of HIP or CIP and extrusion were performed on cryomilled Al–Mg alloys [8, 9, 20, 30, 35–37] and composites [20, 21]. The microstructure of a cryomilled 5083 Al processed

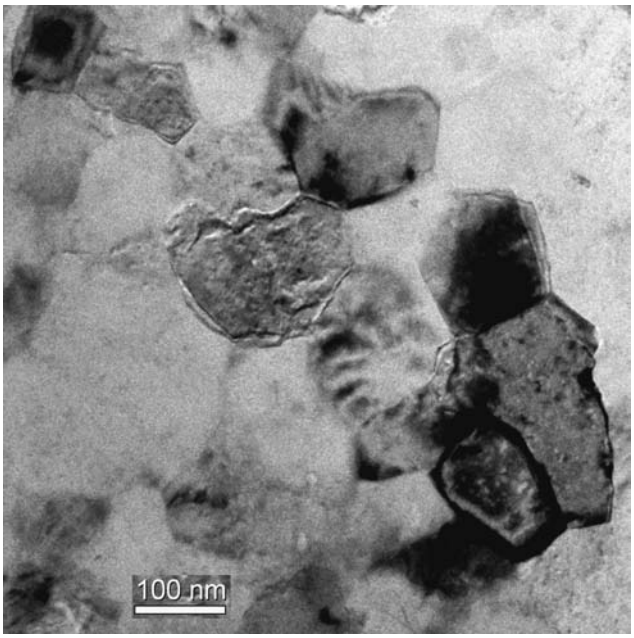

Fig. 6 Microstructure of a cryomilled 5083 Al processed via CIP and extrusion [38]

via CIP and extrusion is shown in Fig. 6 [38]. The average grain size of 200 nm in cryomilled 5083 Al regions is obtained. Grain growth during the subsequent extrusion step is relatively small because of the relatively short time involved as compared to that used in HIP. Therefore, the microstructure after CIP and extrusion in cryomilled Al alloys is generally homogeneous.

The chemical composition of five bulk cryomilled Al alloys is listed in Table 1. The cryomilled Al alloys usually contain various extraneous elements, in addition to their alloying elements. Iron, nickel, chromium and manganese are contaminants from the milling media (stainless steel balls and vial) used in the milling process. Nitrogen, oxygen, carbon and hydrogen are introduced into the material from the process control agent (0.2–0.3 wt. pct of stearic acid $CH_3(CH_2)_{16}CO_2H$) that is frequently used during cryomilling. Silicon, copper, zinc and titanium probably originate from the starting material powders. Similar types, but higher levels, of contamination occur when composite materials with hard reinforcements are cryomilled [19]. The existence of contamination elements can influence both the microstructure and the mechanical performance of the cryomilled Al alloys [37].

In the following sections, the microstructural stability and mechanical properties of cryomilled materials are discussed.

Thermal stability of cryomilled Al alloys

A high thermal stability of a cryomilled 5083 Al alloy processed via HIP and extrusion is evident from microstructure studies after creep tests at two temperatures: 573 and 623 K [39]. An average grain size of 200 nm was observed in the microstructure of the cryomilled 5083 Al. After a long time exposure for nearly 1000 h at temperatures of 573 and 623 K (0.61–0.66 T_m, where T_m is the melting temperature of the material in Kelvin scale), there is only slight grain growth. An average grain size of approximately 220 nm and an average grain size of approximately 280 nm were observed after holding for 996 h at a temperature of 573 K and 938 h at a temperature of 623 K, respectively. After holding at elevated temperatures, however, extremely fine precipitates of approximately 20~50 nm were observed. As discussed in the preceding sections, after mechanically alloying in liquid nitrogen, most of the alloying elements are essentially dissolved into the aluminum matrix, forming a supersaturated solid solution [8, 16, 36]. Small amounts of impurity elements (O, N, C, H, Fe, Cr, etc.) are also introduced into the aluminum alloy during cryomilling processing, with some of them forming nanoscale dispersions [6]. The above effects enhance the retarding force on grain-boundary migration. The existence of second phases (nanoscale aluminum oxide, nitride, carbide, or precipitates), in combination with grain boundary segregation of solute and/or impurity elements is considered to play a significant role in stabilizing the microstructure.

Table 1 Chemical composition of cryomilled Al alloys

Materials (wt.%)	Elements (wt.%)									Refs.
	O	N	C	Fe	Cr	Mn	Ni	Si	Cu	
Al–5.05Mg–0.59Mn	0.41	0.16	0.132	0.2	0.13	0.59	0.16	–	–	[6]
Al–4.23Mg–0.67Mn	0.45	0.71	0.197	0.27	0.081	0.67	0.008	0.16	0.077	[39]
Al–5.24Mg–0.51Mn	0.31	0.37	0.164	0.25	0.017	0.51	<0.002	0.52	0.061	[40]
Al–6.91Mg	0.28	0.38	0.111	0.12	0.004	0.0027	0.012	0.11	0.044	[8]
Al–7.37Mg–0.21Sc	0.3	0.3	0.157	0.055	0.014	0.003	0.014	0.049	0.005	[36]

In a recent study, thermal stability of a cryomilled 5083 Al alloy was analyzed [40]. The bulk cryomilled 5083 Al with an average grain size of 305 nm was investigated in the temperature range of 473–673 K for different annealing times of 1–50 h, as shown in Fig. 7. Appreciable grain growth was observed at temperatures of >573 K, whereas there was limited grain growth at temperatures <573 K even after long annealing times. Preliminary studies on cryomilled 5083 Al composites indicate that the introduction of hard particle reinforcements does not affect the thermal stability of the alloy matrix, even when the reinforcement is in the nanometer size range [20, 41].

The kinetics of grain growth is often expressed by the following form [42]:

$$D^n - D_o^n = kt \tag{2}$$

where D is the average instantaneous grain size, D_o is the initial grain size, n is the grain growth exponent, t is the annealing time, and k is a rate constant that depends on the temperature but is insensitive to the grain size. Thus, k usually can be expressed by Arrhenius equation:

$$k = k_o \exp\left(\frac{-Q}{RT}\right) \tag{3}$$

where k_o is a constant, Q is the activation energy for grain growth and R is the molar gas constant. By differentiating Eq. 2, the isothermal rate of the grain growth can be represented by

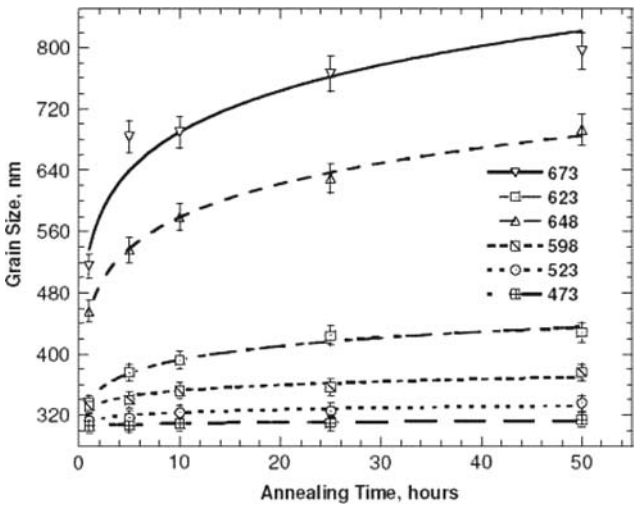

Fig. 7 The grain size as a function of annealing time at different annealing temperature of a cryomilled 5083 Al alloy [40]

$$\frac{dD}{dt} = \frac{k}{n}\left(\frac{1}{D}\right)^{n-1} \tag{4}$$

The value of n can be estimated from the slope of straight line of log (dD/dt)–log ($1/D$). It is observed that the grain growth exponent, n, decreases from 23 to 9.4 with the increase of annealing temperature from 473 to 673 K [40]. The values of the grain growth exponent, n, deduced from the grain growth data are higher than the value of 2 predicted from elementary grain growth theories. The discrepancy was attributed to the operation of strong pinning forces on boundaries during the annealing treatment in the cryomilled 5083 Al alloy, which is most likely related to the presence of dispersion particles, which are mostly introduced during cryomilling [40].

For materials containing dispersion particles, Burke developed a model of grain growth based on the drag forces exerted by the dispersion particles on the migrating grain boundaries [43]. In his model, it is considered that the grain growth rate is controlled by the decreasing difference between the ultimate limiting grain size and the changing value of the instantaneous grain size, rather than by the instantaneous grain size. Burke's model may be expressed by the following equation:

$$\frac{D_o - D}{D_m} + \ln\left(\frac{D_m - D_o}{D_m - D}\right) = \frac{k_o t}{D_m^2}\exp\left(\frac{-Q}{RT}\right) \tag{5}$$

where D_m is the limiting ultimate grain size for the particular annealing temperature. In his model, Burke has assumed that the drag force is independent of grain size. As indicated by Michels et al. [44], such an assumption is reasonable under the condition that the source of pinning does not depend on grain size. This situation exists when dispersion particles or pores produce pinning. By differentiating Eq. 5, the following growth rate equation is obtained:

$$\frac{dD}{dt} = k\left(\frac{1}{D} - \frac{1}{D_m}\right) \tag{6}$$

From the linear plot of dD/dt–$1/D$, the value of slope (k) at the different annealing temperature can be determined. Using Eq. 2, the value of activation energy for grain growth can be determined from the plot of $\ln(k)$ as a function of $1000/RT$ [40]. From values of activation energy for grain growth, two-grain growth regimes were identified: the low-temperature region (<573 K) and the high-temperature region (>573 K). For temperatures lower than 573 K, the value of

activation energy of 25 ± 5 kJ/mol was determined. It is suggested that this low activation energy represents the energy for the reordering of grain boundaries in the UFG material. For temperatures higher than 573 K, the value of activation energy of 124 ± 5 kJ/mol was measured. This value of activation energy, 124 ± 5 kJ/mol, lies between that for grain boundary diffusion and lattice diffusion in analogous aluminum polycrystalline systems [40].

Mechanical properties of cryomilled materials

Figure 8a shows the plots of true tensile stress as a function of true strain of four 5083 Al alloys, i.e., a cryomilled 5083 Al alloy consolidated via CIP and extrusion with an average grain size of approximately 150–200 nm [9, 38], a cryomilled 5083 Al alloy consolidated via HIP and extrusion with the mean grain size of about 500 nm (Han and Lavernia, unpublished data, 2003), a cryomilled bimodal 5083 Al alloy [6], and a coarse-grained 5083 Al [45]. The cryomilled bimodal 5083 Al alloy [6] is reported to possess small grains of about 30 nm, and some large grains of approximately several hundred nanometers in microstructure after extrusion at elevated temperatures. The coarse-grained 5083 Al alloy has a grain size of 200 μm [45]. The highest value of yield strength of 713 MPa is observed in the cryomilled 5083 Al alloy consolidated via CIP and extrusion. Such a high strength is mostly attributed

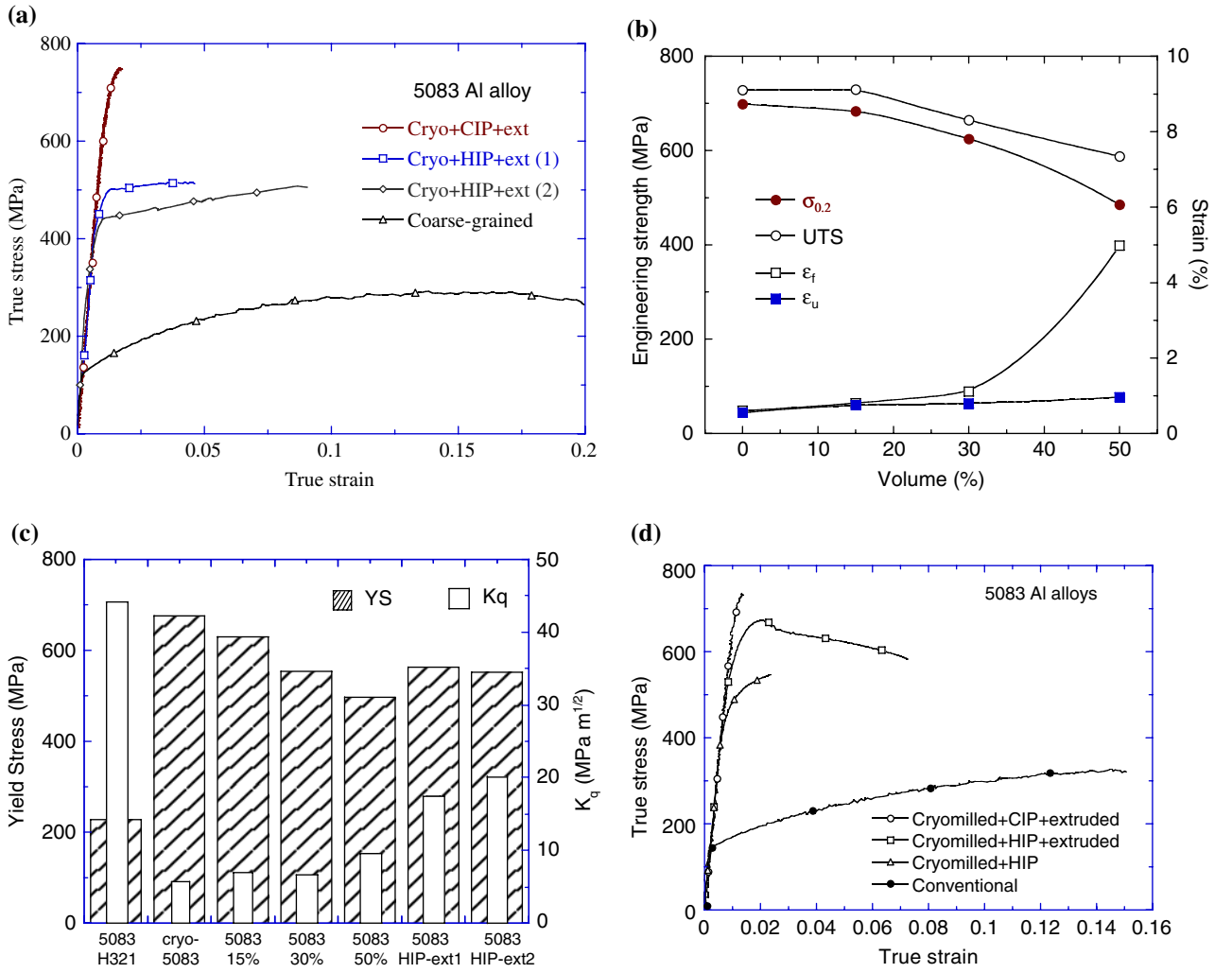

Fig. 8 (**a**) True tensile stress as a function of true strain of cryomilled 5083Al alloys (CIP + ext) [9] and cryomilled 5083 Al (HIP + ext1) (Han and Lavernia, unpublished data 2003), cryomilled 5083 Al (HIP + ext2) [6] and coarse 5083 Al alloys [45]). (**b**) Tensile stress as a function of strain of bimodal cryomilled Al 5083 alloys [9]. (**c**) Comparison of yield strength (shadow column) and fracture toughness (open column) of cryomilled 5083 Al alloys [49] with those of conventional 5083 Al. (**d**) True tensile stress as a function of true strain of a cryomilled 5083 Al consolidated via CIP and extrusion [9], and a cryomilled 5083 Al consolidated via HIP and extrusion [50], a cryomilled 5083 Al consolidated via HIP [50], and a conventional 5083 Al [8]

to the grain size effect compared to other 5083 Al alloys. However, an extremely low ductility of 0.3% is observed in the cryomilled 5083 Al alloy consolidated via CIP and extrusion. It appears that ductility in cryomilled Al alloys decreases with decreasing grain size, same as observed in many other nanostructured materials.

Large increases in strength are frequently reported for nanostructured metals, a phenomenon that is explained in part by grain refinement and the well-known Hall–Petch relationship. However, low ductility is a serious deficiency in most of these materials [46]. Low ductility, and the associated loss of toughness, reduces the potential for engineering application. Inspection of the relevant literature reveals that a number of approaches have been proposed in an effort to enhance the ductility of nanostructured materials [6, 47]. In earlier studies, Tellkamp and co-workers reported on the mechanical properties of a nanostructured cryomilled 5083 Al alloy, with a yield strength of 334 MPa, ultimate strength of 462 MPa and an elongation of 8.4% [6]. In this study, it was suggested that the presence of coarse grains was responsible for the observed ductility. The coarse grains arose as a result of thermomechanical processing of the nanostructured powders, i.e., consolidation and extrusion. More recently, enhancement of ductility in cryomilled materials has been accomplished via the introduction of a bimodal microstructure [9, 48]. For instance, the cryomilled 5083 Al alloys with 15% unmilled coarse grains (CG), 30% CG and 50% CG are processed by the same procedures of CIP and extrusion as those in above cryomilled 5083 Al alloy [9]. In the consolidated material, there are both the nanostructured regions with grain sizes of 100–300 nm and larger grained bands, originating from the unmilled powder, which have a grain size of ~500 nm–1 μm. There is a trend of decreasing strength and increasing elongation with an increasing fraction of micron-grain material, as shown in Fig. 8b. The bimodal cryomilled Al alloys show an improved ductility without much decrease in strength. The bimodal microstructure in cryomilled Al alloys also leads to an enhancement of fracture toughness. Figure 8c compares the strength and fracture toughness of several cryomilled 5083 Al alloys [49] with those of conventional 5083 Al alloy (a benchmark material). The cryomilled 5083 Al alloy is processed by CIP and followed by extrusion [9]. The cryomilled 5083 Al alloy (HIP and ext1) and the cryomilled 5083 Al alloy (HIP and ext2) are processed by HIP and followed by extrusion at temperatures of 473 and 498 K, respectively [34]. As shown in Fig. 8c, the cryomilled 5083 Al alloy has a much higher strength, but with a low fracture toughness. With increasing volume fraction of coarse grains, the fracture toughness of bimodal 5083 Al alloys increases. It is worth noting that the values of fracture toughness of cryomilled 5083 Al alloys processed by HIP and extrusion are also high compared to those processed by CIP and extrusion. The intrinsic bimodal microstructure that evolves during HIP gives a better combination of strength, ductility and toughness than that given by the consolidation of mixture of cryomilled and unmilled powders by CIP. This may imply that the interfacial bonding fostered during HIP is strong.

The mechanical behavior in the form of tensile true stress as a function of true strain of four 5083 Al alloys, i.e., a cryomilled nanostructured 5083 Al alloy consolidated via CIP and extrusion [9], and a cryomilled nanostructured 5083 Al alloy consolidated via HIP and extrusion [50], a cryomilled nanostructured 5083 Al alloy consolidated via HIP [50], and a conventional 5083 Al [8], is shown in Fig. 8d. The highest value of yield strength of 713 MPa, however, an extremely low ductility of 0.3%, is observed in the cryomilled 5083 Al alloy consolidated via CIP and extrusion. The cryomilled 5083 Al alloy consolidated by HIP has a smaller grain size, but both strength and ductility are lower than those of cryomilled 5083 Al alloy consolidated via HIP and extrusion. The poor mechanical performance of the former cryomilled 5083 Al alloy may be attributed to the residual porosity or poor interfacial bonding in the HIP microstructure. Both a high strength and a high ductility are observed in the cryomilled 5083 Al alloy consolidated via HIP and extrusion. The good combination of mechanical properties is attributed to the intrinsic bimodal microstructure, which is introduced during HIP. Obviously, there is a significant influence of consolidation routes on the properties of cryomilled 5083 Al alloys.

Recently, an Al–5%Mg alloy was processed by a modified cryomilling processing [51], in which the liquid nitrogen flows around the vial to cool the milling process rather than flows into the vial to form a liquid nitrogen slurry during milling. In addition, the Al–Mg alloy powders were joined together to form several small balls, without a need for consolidation. Inspection of chemical composition indicates that there are similar levels of O and Fe by this small scale milling to those by large scale milling as those reported in Table 1. Because of the lack of consolidation steps, the average grain size of 26 nm after milling was reported. It is interesting to note that there are both high strength (tensile yield strength of 612 MPa) and good ductility (ductility of 8.5%) from their stress–strain curves by using a miniaturized tensile specimen

[51]. Although the in situ consolidated Al–Mg alloy with the grain size of 26 nm has a strength level similar to the cryomilled Al alloys consolidated by HIP or CIP and extrusion with the grain size of 200 nm, it has much higher tensile ductility. The high ductility is attributed to the much fewer artifacts in the in situ consolidated Al–Mg alloy [51].

Recently, a cryomilled 5083 Al composite with a tri-modal microstructure was processed [20]. The tri-modal composite consists of 10% B_4C particle, 50% unmilled coarse-grained 5083 Al and the balance nanostructured 5083 Al. It is interesting to note that there is high yield strength of 1065 MPa. In addition, a relatively straight elastic deformation line was observed, without an evidence of micro-yielding, although it is expected in the stress–strain behavior under compressive load, because the unmilled coarse-grained 5083 Al yields at a stress below 300 MPa. This unique phenomenon can be explained in terms of the load transfer associated with the tri-modal microstructure. The applied load on the coarse-grained Al can be effectively transferred to the nanocrystalline Al, because a good interface between the coarse-grained Al and the nanocrystalline Al can easily be developed during consolidation due to the same chemical composition in both regions. In the tri-modal composite, however, the load applied on the nanocrystalline Al can be further transferred to the stronger B_4C particles, because a good interface between the nanocrystalline Al and the B_4C can be formed during cryomilling. As a consequence, most of the applied load is sustained by the nanocrystalline Al and the B_4C particles and only a small fraction of the load remains in the coarse-grained Al, which is insufficient to cause yielding. In summary, the load transfer that occurred in the tri-modal composite behaves like a ''relay race'', from the coarse-grained Al to the nanocrystalline Al and then to the B_4C particles. Consequently, most of the applied load is sustained by the B_4C particles, resulting in a material with extremely high yield strength [20].

Discussion

Strengthening mechanisms

The reported high strength in cryomilled materials could be the result of the contributions of several types of strengthening mechanisms, such as grain size effect, solid-solution hardening, dispersion strengthening, and precipitate strengthening, etc. On the basis of the Hall–Petch relationship ($\sigma_d = \sigma_o + k_y \cdot d^{1/2}$, where σ_o is a frictional stress required to move dislocations and k_y is the locking parameter), there is an increase in strength with a decrease in grain size [52]. The grain size effect was considered to play a significant role in the strengthening of cryomilled Al alloys and composites [8, 20, 36]. A second contribution to strength in nanostructured materials may arise from solid solution strengthening. Ball milling usually extends the solid solubility of solute elements [2], thus leading to the larger solid solution strengthening than that in conventional materials. This contribution to strengthening can be estimated, to a first approximation, from the following expression [53]: $\Delta\sigma_{ss} = 2\sqrt{2}(0.2)^{3/2} G\delta^{3/2} c^{1/2}$ where G is the shear modulus of the matrix, δ is the mismatch parameter and c is the atomic fraction concentration of the solute. A third contribution to strength in nanostructured materials that may arise involves strong interactions of dislocations with dispersoids or precipitates, i.e., Orowan strengthening, which is dependent on the volume fraction and interparticle distance of particles. In addition to above mentioned strengthening mechanisms, the composite strengthening exists in the nanostructured composites consolidated from milled powders [20]. For the discontinuously reinforcements, the rule of mixtures ($\sigma_c = \sigma_m(1–f) + \sigma_r f$) is used to estimate the strength of nanostructured composites, where σ_c, σ_m and σ_r are the yield strength of the composite, matrix and reinforcement, respectively, and f is the volume fraction of the reinforcement. Because of the improvement in the reinforcement–matrix interface and the homogeneity of the reinforcement within the matrix, however, the behavior observed in the composites made from cryomilled powders is not fully explained by this rule [20].

Work softening

After yielding, there is a phenomenon of a stress-drop, which is frequently observed in nanostructured materials. Nanostructured materials processed via consolidation of milled powders usually contain contamination elements and nanoscale dispersoids that are generated during milling. For example, nanostructured Al alloys processed via cryomilling processing usually contain other elements, in addition to their alloying elements [6, 36]. The existence of extraneous elements and nanoscale dispersoids influences both the microstructure and the mechanical performance of the cryomilled Al alloys. One possible explanation for the phenomenon of stress-drop is the detachment of dislocations from ultrafine oxide or nitride dispersoids in materials consolidated from milled powders [8, 54]. Dislocations can accumulate around ultrafine dispersoids during

plastic deformation. When dislocations burst out from nanometric dispersoids under high applied stresses or annihilate each other in the vicinity of dispersoids, a stress-drop can occur in the stress–strain curve [8]. A similar stress drop phenomenon has been observed in other UFG materials consolidated from milled powders [54–56], and has been attributed to the collective movement of large numbers of mobile dislocations that were previously pinned by a complex network of fine dislocation cells. The subsequent flow stress plateau was attributed to the reduced resistance to glide of unpinned dislocations [55]. The above-mentioned stress drop phenomenon has been associated with the initiation of Lüders bands in cryomilled Al alloys [9]. During Lüders band formation, subsequent plastic deformation is observed to accelerate on one side of the Lüders band. In addition, propagation of the Lüders band is limited by the presence of glide obstacles and does not extend across the gage section of the alloys as it does in conventional materials. Therefore, it has been proposed that the deformation strain that follows the attainment of the peak stress in cryomilled nanostructured Al alloys is principally related to the formation and propagation of Lüders strain [9].

Following the initiation of Lüders band or necking, the phenomenon of low strain hardening or work softening behavior is often observed in the stress–strain curves, which is another characteristic that is often observed in nanostructured or UFG Al alloys [6, 36, 54–61]. Although the underlying mechanisms of the low strain hardening or work softening behavior are not fully understood, three possible explanations can be offered as follows.

First, in an investigation of MA Al alloys, the work softening behavior was rationalized on the basis of a modified theory of low energy dislocation structure (LEDS) [55, 62]. In this study, it was proposed that the work softening was accomplished via a reduction of dislocation density or a reduction of the Hall–Petch strengthening effect. It is quite likely that during the course of mechanically alloying, exceptionally high dislocation densities may have been introduced. In fact, high dislocation densities, on the order of $1.3{\cdot}10^{17}$ m^{-2}, are indeed observed in cryomilled Al–Mg powders with a grain size of ~25 nm [5, 15]. After consolidation, the dislocation densities in cryomilled Al alloys may remain high, since dislocations are likely to be stabilized via interactions with nanometric particles; such dislocation/particle interactions have been documented for a variety of systems [36, 55, 63]. The dislocation densities in the dispersion-strengthened materials might be higher than those in dispersoid-free materials. Therefore, subsequent plastic deformation will cause the dislocation density to be reduced to the equilibrium status and thus the flow stress will not increase, since every new glide dislocation loop will give rise to the annihilation of more than its own length, resulting in work softening behavior [55]. Work softening may also be related to a reduction in the friction stress of the Hall–Petch strengthening during the unlocking of dislocations from impurity or alloying atmospheres, and/or during the breaking of barriers in grain or dislocation structures [64].

Secondly, an alternative explanation for the observed low strain hardening or work softening behavior is the occurrence of dynamic recovery during plastic deformation [8, 64]. Mobile dislocations can be trapped by both impenetrable obstacles and forest dislocations, forming additional obstacles to glide that contribute to strain hardening. On the other hand, immobile dislocations may be annihilated due to cross-slip or rearrange to form sub-boundaries of relatively low energy, contributing to dynamic recovery [65, 66]. In a related study of the tensile and compressive behavior of UFG AlFeVSi alloy, it was proposed that dynamic recovery occurs in the low-strain-hardening region [67]. Although solute additions usually retard dynamic recovery by increasing lattice frictional stress and thereby inhibiting dislocation slip, a high disorder region, as well as the associated high vacancy concentration in cryomilled Al alloys may facilitate recovery, causing low strain hardening and a relatively high ductility.

Lastly, the activation volumes of cryomilled Al alloys were recently calculated from strain rate jump tests and relatively low values were observed [68]. The low values of activation volume during plastic deformation suggest that dislocations do not accumulate within the grains but glide to grain boundaries, resulting in the elastic–perfectly plastic behavior of cryomilled Al alloys [68].

The role of bimodal structure

The mechanisms of enhancement of ductility in bimodal cryomilled materials have also been investigated in recent studies [9, 69]. The microstructure of bimodal cryomilled materials processed after extrusion is analogous to short-fiber metal matrix composites, in that the submicron-grained bands are distributed parallel to the extrusion direction. Several toughening mechanisms have been proposed to explain ductile-phase toughening of composite microstructures, such as crack bridging, crack blunting, crack deflection, stress distribution of crack tip, crack front convolution and local plane stress deformation, etc. [70, 71]. On the

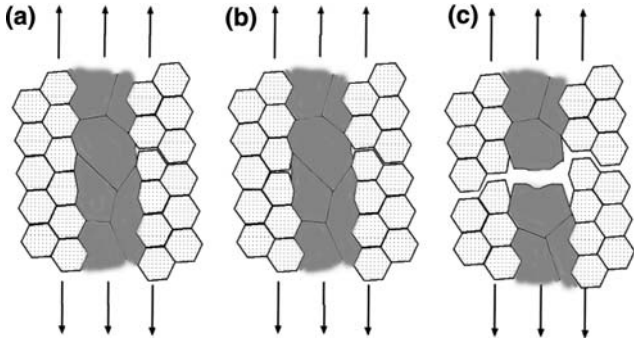

Fig. 9 Delamination and bridging mechanisms in a bimodal microstructure [9]

basis of microstructural characteristics of bimodal cryomilled materials, a model of crack bridging combined with the concept of delamination has been developed, as illustrated in Fig. 9 [9]. The figure shows the propagation of a micro-crack in a nanostructured material with a bimodal lamellar structure. In the bimodal Al alloys, microcracks are expected to nucleate first in the harder nanostructured regions and propagate along grain boundaries. When a microcrack meets a submicron-grained band, the band will retard propagation by blunting the crack and/or by delamination of interfaces between submicron-grained and nanostructured-grain regions, as shown in Fig. 9a. When more dislocations are emitted into the submicron grain, a new slip surface may be formed, eventually leading to necking and cavitation within the submicron-grained bands, as shown in Fig. 9b. Finally, dimples on the submicron-grained regions and delamination at interfaces will be generated on fracture surface (as revealed in Fig. 9c). The delamination at interfaces and the necking deformation of ductile submicron-grain regions will cause significant energy loss, resulting in an enhanced tensile ductility.

Summary and conclusions

Cryomilling processing for nanostructured or ultrafine-grained metallic materials is reviewed. During ball milling, the materials experience repeated severe plastic deformation, which leads to the grain refinement and eventually the formation of nanostructured grains. Cryomilling, which is conducted in a cryogen (usually liquid nitrogen) slurry or at a cryogen temperature, takes advantage of both the extremely low cryogen temperature and the advantages that are provided with conventional mechanical milling. The extremely low milling temperature in cryomilling suppresses the recovery and recrystallization and leads to finer grain structures and more rapid grain refinement. The milling time used for metal matrix composites was shorter than that needed with normal mechanical milling which is extensively applied to fabricate nanocrystalline metallic materials. In addition, there is a homogeneous distribution of the reinforcement and good matrix/reinforcement interfaces in metal matrix composites processed by cryomilling.

Conventional powder metallurgy processes such as hot isostatic pressing have been used as the primary consolidation approach for bulk nanostructured materials. After the primary processing of isostatic pressing, a secondary process such as extrusion or forging can be applied to remove residual porosity and improve mechanical properties. The consolidation conditions have a significant effect on mechanical properties of bulk nanostructured materials. Low ductility and low toughness in nanostructured materials can be overcome by adding submicron grains into nanostructured region for the formation of bimodal microstructures. The high strength is primary attributed to the grain size effect by the Hall–Petch relation, solid solution hardening and Orowan dispersion strengthening. The low strain hardening behavior in nanostructured materials processed by milling can be attributed to dislocation annihilation or dynamic recovery during plastic deformation. Low ductility in cryomilled materials can be overcome by adding submicron grains into the nanostructured region for the formation of bimodal microstructures. The delamination at interfaces and the necking deformation of ductile submicron-grain regions in bimodal cryomilled materials will cause significant energy loss, resulting in an enhanced tensile ductility.

Acknowledgements Financial support from the Office of Naval Research (Grant No. N00014-04-1-0370) and US Marine Corps (Contract No. N00014-03-C-0163) is gratefully acknowledged.

References

1. Koch CC (ed) (2002) Nanostructured materials: processing, properties and potential applications. Noyes Publications (William Andrew Publishing), Norwich, NY
2. Suryanarayana C (2001) Prog Mater Sci 46:1
3. Luton MJ, Jayanth CS, Disko MM, Matras S, Vallone J (1989) In: Materials Research Society (ed) MRS Proc, vol 132, p 79
4. Perez RJ, Jiang HG, Dogan CP, Lavernia EJ (1998) Metall Mater Trans A 29A:2469
5. Zhou F, Liao XZ, Zhu YT, Dallek S, Lavernia EJ (2003) Acta Mater 51:2777
6. Tellkamp VL, Melmed A, Lavernia EJ (2001) Metall Mater Trans A 32A:2335

7. Rodriguez R, Hayes RW, Berbon PB, Lavernia EJ (2003) Acta Mater 51:911
8. Han BQ, Lee Z, Nutt SR, Lavernia EJ, Mohamed FA (2003) Metall Mater Trans A 34A:603
9. Han BQ, Lee Z, Witkin D, Nutt SR, Lavernia EJ (2005) Metall Mater Trans A 36A:957
10. Youssef KM, Scattergood RO, Murty KL, Koch CC (2004) Appl Phys Lett 85:929
11. Fecht HJ (1995) NanoStruct Mater 6:33
12. Benjamin JS, Volin TE (1974) Metall Trans A 5:1929
13. Mautice DR, Courtney TH (1990) Metall Trans A 21:289
14. Mautice DR, Courtney TH (1995) Metall Mater Trans A 26:2437
15. Liao XZ, Huang JY, Zhu YT, Zhou F, Lavernia EJ (2003) Philos Magn A 83:3065
16. Zhou F, Rodriguez R, Lavernia EJ (2002) Mater Sci Forum 386–388:409
17. Eckert J, Holzer JC, Krill ICE, Johnson WL (1992) J Mater Res 7:1751
18. Mohamed FA (2003) Acta Mater 51:4107
19. Ye J, He J, Schoenung JM (2006) Metall Mater Trans A (in print)
20. Ye J, Han BQ, Lee Z, Ahn B, Nutt SR, Schoenung JM (2005) Scr Mater 53:481
21. Tang F, Hagiwara M, Schoenung JM (2005) Scr Mater 53:619
22. Chung KH, He J, Shin DH, Schoenung JM (2003) Mater Sci Eng A 356:23
23. Fogagnolo JB, Ruiz-Navas EM, Robert MH, Torralba JM (2002) Scr Mater 47:243
24. Groza JR, Dowding RJ (1996) NanoStruct Mater 7:749
25. Bourell DL, Groza JR (2002) ASM handbook vol 7—Powder metal technologies and applications, vol 7. ASM International, Materials Park, OH
26. Groza JR (2002) Nanostructured materials: processing, properties and potential applications. Noyes Publications, Norwich, New York, p 115
27. Ashby MF (1991) Powder metallurgy: an overview. The Institute of Metals, London, p 144
28. Atkinson HV, Davies S (2000) Metall Mater Trans A 31A:2981
29. Lee Z, Rodriguez R, Hayes RW, Lavernia EJ, Nutt SR (2003) Metall Mater Trans A 34A:1473
30. Zhang Z, Han BQ, Witkin D, Ajdelsztajn L, Lavernia EJ (2006) Scr Mater 54:869
31. Lynn-Ferguson B, Smith OD (1984) ASM handbook vol 7—Powder metallurgy, vol 7. ASM International, Materials Park, p 537
32. Anderson RL, Groza J (1988) Metal Powder Report 43:678
33. Chan HW (1988) Mater Design 9:355
34. Witkin D, Han BQ, Lavernia EJ (2005) J Mater Res 20:2117
35. Park YS, Chung KH, Kim NJ, Lavernia EJ (2004) Mater Sci Eng A 374:211
36. Han BQ, Lavernia EJ, Mohamed FA (2005) Metall Mater Trans A 36A:345
37. Witkin DB, Lavernia EJ (2006) Prog Mater Sci 51:1
38. Han BQ, Huang JY, Zhu YT, Lavernia EJ (2006) Scr Mater 54:1175
39. Han BQ, Zhang Z, Lavernia EJ (2005) Philos Magn Lett 85:97
40. Roy I, Chauhan M, Mohamed FA (2006) Metall Mater Trans A 37A:721
41. Tang F, Schoenung JM (2006) A paper in preparation
42. Beck PA, Kremer JC, Demer LJ, Holzworth ML (1948) Trans TMS-AIME 175:372
43. Burke JE (1949) Trans TMS-AIME 180:73
44. Michels A, Krill CE, Ehrhardt H, Birringer R, Wu DT (1999) Acta Mater 47:2143
45. Chang SY, Lee JG, Park KT, Shin DH (2001) Mater Trans 42:1074
46. Koch CC, Morris DG, Lu K, Inoue A (1999) MRS Bull 24:54
47. Wang Y, Chen M, Zhou F, Ma E (2002) Nature 419:912
48. Witkin D, Lee Z, Rodriguez R, Nutt S, Lavernia E (2003) Scr Mater 49:297
49. Pao PS (2005) Unpublished data on fracture toughness of cryomilled Al alloys
50. Witkin D, Han BQ, Lavernia EJ (2006) Metall Mater Trans A 37A:185
51. Youssef KM, Scattergood RO, Murty KL, Koch CC (2006) Scr Mater 54:251
52. Weertman JR (1993) Mater Sci Eng A166:161
53. Hull D, Bacon DJ (1984) Introduction to dislocations. Pergamon Press, Oxford
54. Kim YW, Bidwell LR (1982) Scr Metall 16:799
55. Wilsdorf HGF, Kuhlmann-Wilsdorf D (1993) Mater Sci Eng A164:1
56. Last HR, Garrett RK (1996) Metall Mater Trans A 27A:737
57. Mukai T, Kawazoe M, Higashi K (1998) NanoStructured Mater 10:755
58. Hayes RW, Rodriguez R, Lavernia EJ (2001) Acta Mater 49:4055
59. Hasegawa T, Miura T, Takahashi T, Yakou T (1992) ISIJ Int 32:902
60. Sun XK, Cong HT, Sun M, Yang MC (2000) Metall Mater Trans A 31A:1017
61. Champion Y, Langlois C, Guerin-Mailly S, Langlois P, Bonnentien J-L, Hytch MJ (2003) Science 300:310
62. Kuhlmann-Wilsdorf D, Wilsdorf HGF (1992) Phys Status Solidi (a) 172:235
63. Dehiya BS, Weertman JR (1997) In: Earthman JC, Mohamed FA (eds) Creep and fracture of engineering materials and structures. The Minerals, Metals & Materials Society, p 129
64. Kuhlmann-Wilsdorf D (1999) Philos Magn A 79:955
65. Kral R (1996) Phys Status Solidi (a) 157:255
66. Humphreys FJ, Hatherly M (1995) Recrystallization and related annealing phenomena. Pergamon, New York, p 127
67. Hariprasad S, Sastry SML, Jerina KL (1996) Acta Mater 44:383
68. Hayes RW, Witkin D, Zhou F, Lavernia EJ (2004) Acta Mater 52:4259
69. Han BQ, Mohamed FA, Bampton CC, Lavernia EJ (2005) Metall Mater Trans A 36A:2081
70. Lesuer DR, Syn CK, Sherby OD, Wadsworth J, Lewandowski JJ, Hunt JWH (1996) Int Mater Rev 41:169
71. Soboyejo W (2003) Mechanical properties of engineered materials. Marcel Dekker, Inc., New York, p 583